Effect of magnetism and light sp-dopants on chain creation in Ir and Pt break junctions

2014 J. Phys.: Condens. Matter 26 295302

(http://iopscience.iop.org/0953-8984/26/29/295302)

IOP Publishing Journal of Physics: Condensed Matter
J. Phys.: Condens. Matter **26** (2014) 295302 (9pp) doi:10.1088/0953-8984/26/29/295302

Effect of magnetism and light sp-dopants on chain creation in Ir and Pt break junctions

S Di Napoli[1,2], A Thiess[3], S Blügel[3] and Y Mokrousov[3]

[1] Departamento de Física de la Materia Condensada, CAC-CNEA, Avenida General Paz 1499, (1650) San Martín, Pcia. de Buenos Aires, Argentina
[2] Consejo Nacional de Investigaciones Científicas y Técnicas, CONICET, Buenos Aires, Argentina
[3] Peter Grünberg Institut and Institute for Advanced Simulation, Forschungszentrum Jülich and JARA, D-52425 Jülich, Germany

E-mail: dinapoli@tandar.cnea.gov.ar

Received 6 February 2014, revised 29 April 2014
Accepted for publication 27 May 2014
Published 25 June 2014

Abstract
Applying the generalization of the model for chain formation in break-junctions (Di Napoli *et al* 2012 *J. Phys.: Condens. Matter* **24** 135501), we study the effect of light impurities on the energetics and elongation properties of Pt and Ir chains. Our model enables us to develop a tool ideal for detailed analysis of impurity-assisted chain formation, in which zigzag bonds play an important role. In particular we focus on H (s-like) and O (p-like) impurities and assume, for simplicity, that the presence of impurity atoms in experiments results in a ..M-X-M-X-... (M: metal, X: impurity) chain structure in between the metallic leads. Feeding our model with material-specific parameters from systematic full-potential first-principles calculations, we find that the presence of such impurities strongly affects the binding properties of the chains. We find that, while both types of impurities enhance the probability of chains being elongated, the s-like impurities lower the chain's stability. We also analyze the effect of magnetism and spin-orbit interaction on the growth properties of the chains.

Keywords: low dimensional systems, *ab initio* calculations, atomic chains, break junctions

(Some figures may appear in colour only in the online journal)

1. Introduction

The elongation of some metal junctions allows the fabrication of self-supported one-dimensional systems: the suspended atomic chains, achieved, for example, in a mechanically controllable break junction (MCBJ) [1]. In such an experiment a metallic junction which has been created by lithography is being stretched until it breaks. If this stretching is performed in a controllable way by using piezoelements then the creation of stable monowires can be observed. With this technique it has been possible to create monoatomic chains from Ir [2], Pt [1] and Au [3–5] up to a length of 5–6 atoms for Pt, and even more for Au, which has been confirmed by measuring conductance during formation. One of the most exciting perspectives in this area is the ability to study, not only theoretically but also experimentally, some of the most fundamental properties of one-dimensional systems, which are mostly related to their transport properties. As magnetism is enhanced in such systems, the latter are promising candidates for spintronics applications due to the ability to simultaneously probe, control and switch the magnetic state by spin-polarized electrical currents [6–10].

Since the creation of the first free-standing atomic chains of gold atoms in 1998 [1, 3], a lot of work has been done in the search for other elements that could also form atomic chains. Although there have been some reports on the formation of several 3d- and 4d-row metallic chains, it has not been definitely established whether it is possible to successfully create long atomic chains out of other elements than Au, Pt and Ir. One of the crucial points in the success of chain formation is the reconstruction of the low-index surfaces of the selected elements: gold nanowires spontaneously evolve into freely suspended chains of

atoms. Smit *et al* [1] showed that all the 5d metals that present similar reconstructions (Ir, Pt and Au) also form chains of atoms.

In the last few years it has been possible to strengthen the bonds in a suspended chain and achieve a higher probability of chain producibility by adding external absorbates during the chain formation process. It is known that low-coordinated atoms are chemically more reactive than in bulk [11]. Thus, being the coordination number of only two in an atomic chain, chains are expected to be even more reactive than nanoparticles, which opens up the possibility of molecular absorbates dissociating, even at low temperatures. For instance, O atoms are expected to be incorporated in the chains, as predicted in several previous works [12–16]. Oxygen atoms are not the only kind of impurities that can help in the process of chain formation. There are previous reports on the effect of H, B, C, N and S impurities on gold chains [11, 17, 18]. All of them found that the inserted atoms in gold nanowires form not only stable but also very strong bonds. In a previous work [15], we systematically applied our chain formation model for a detailed study of the trends in the formation of Cu, Ag and Au chains in pure break junctions, as well as Cu, Ag and Au break junctions, with the atmosphere contaminated by H, C, N and O impurities. We also extended the model to the case of a geometrically more complex planar zigzag arrangement of the atoms in the chain. We have demonstrated that adding the mentioned environmental impurities to the noble-metal chain formation process leads to a significantly enhanced probability of chain formation in noble metal break junctions, and that the three considered p-like impurities lead to similar effects, different from the effects found for H impurities. In this work we systematically apply our chain formation model in late 5d transition metals (TMs), namely, Pt and Ir. We consider linear and zigzag arrangements and two prototype impurities, namely s-like (H) and p-like (O). We include spin polarization in all the calculations and carefully check the effect of spin-orbit coupling on our findings. Overall, we find that, in analogy to noble chains, the presence of impurities enhances the probability of chains forming. And while p-like impurities also strengthen the stability of the chains, the s-like impurities enhance the spin moments of the transition metals and lower their structural stability, which is largely dependent on the directional bonding between the atoms due to presence of the d-states at the Fermi energy.

The paper is organized as follows. In the next section a brief description of the computational details used in the calculations is given. In section 3 we present the calculated structural and magnetic properties of the linear and zigzag chains, for both single-atom and chains with impurities. In section 4 the producibility (P-)model is breafly recalled and the results are presented. In this section we also analyze the role of magnetism and spin–orbit coupling in the chain formation process. Finally, we present our conclusions in section 5.

2. Computational details

In the present first-principles calculations, we employ the full-potential linearized augmented plane-wave method for one-dimensional (1D) systems [19], as implemented in the FLEUR code [20]. The calculations are based on density functional theory within the (rev-PBE) generalized gradient approximation (GGA) to the exchange-correlation potential. Basis functions were expanded up to $k_{max} = 4.0$ bohr^{-1} and we have used 32 k points in one half of the 1D Brillouin zone. The position of the boundary between the interstitial and the vacuum region D_{vac}, as well as the in-plane lattice constant $\widetilde{D}$ used for the generation of reciprocal lattice vectors, were set to 8.3 bohr and 9.9 bohr, respectively. For details of the method and spatial partitioning within the 1D FLAPW scheme see [19]. The muffin-tin radii have been set to $R_{MT} = 1.90$ bohr for Pt and Ir (with local orbitals in the 5s and 5p states), and $R_{MT} = 1.0$ bohr for the impurities. These values were chosen, not only to guarantee the good convergence of the obtained results but also to achieve a wide range of zigzag α-angles (see figure 1). For our calculations we included the effect of the spin–orbit interaction, and considered magnetization in the three directions of space (x, y and z), as none of them are equivalent when the zigzag geometry is taken into account.

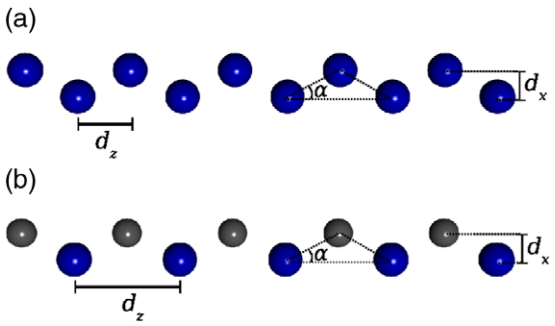

Figure 1. Schematic structure for (*a*) single-atom planar zigzag chains and (*b*) planar zigzag chains with impurities. The infinite zigzag chains make an α-angle with the chain axis, z. d_z is the projection of the metal-to-metal distance into the chain axis, and d_x is the projection into a perpendicular degenerate axis. The metal atoms are represented by large blue spheres, while smaller gray spheres stand for the impurity atoms.

We have set the coordinate system such that the chains are aligned along the z axis, and considered a two-atom unit cell to allow for zigzag arrangements. In figure 1 a schematic picture of the infinite planar zigzag atomic chains is shown, where the defined distances (d_z, d_x), as well as the zigzag α-angle, are presented.

3. Structure and magnetic properties

As one of the main goals of this work is to understand the incidence of the geometric structure, as well as magnetism and spin–orbit interaction in the chain formation process from energetic considerations, we have performed systematic calculations of linear and zigzag geometries for two late 5d TMs, Ir and Pt, with prototype s-like (H) and p-like (O) impurities. We carried out total energy calculations as a function of both interatomic parameters, d_z and d_x, as defined in figure 1. For each of the five chosen d_x distances we performed self-consistent calculations for at least ten different d_z values, fitted each resulting energy curve with a Morse-potential and interpolated the two-dimensional energy profile in the $d_z - d_x$ plane, from

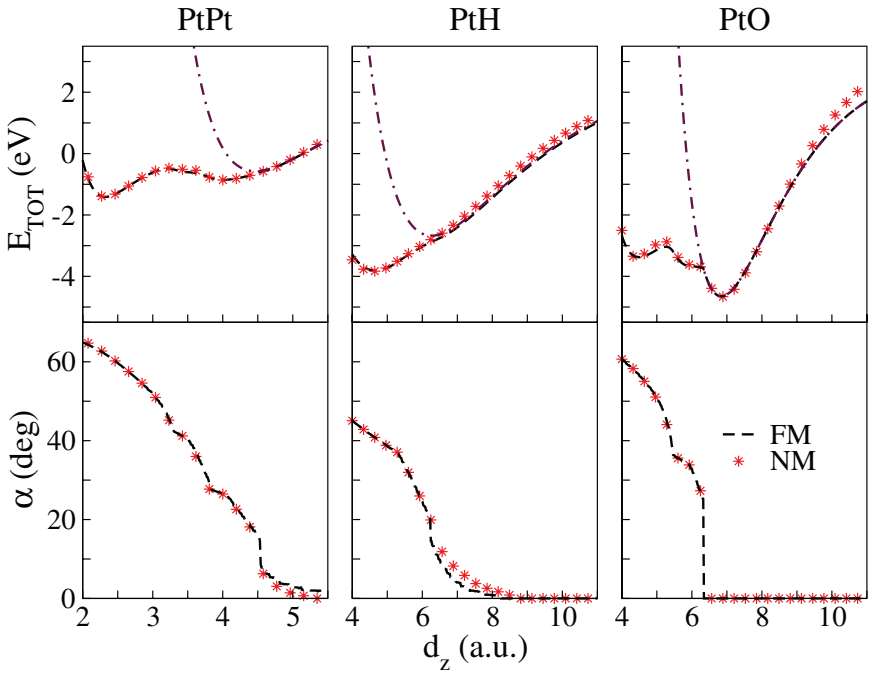

Figure 2. Upper panel: the minimal total energy E_{TOT} (per atom) as a function of the interatomic distance (d_z) for PtPt (left), PtH (middle) and PtO (right). Results of non-magnetic (NM) and ferromagnetic (FM) calculations are presented. The dashed–dotted maroon lines correspond to the total energies of the linear infinite FM chains. Lower panel: the evolution of the corresponding zigzag α-angles.

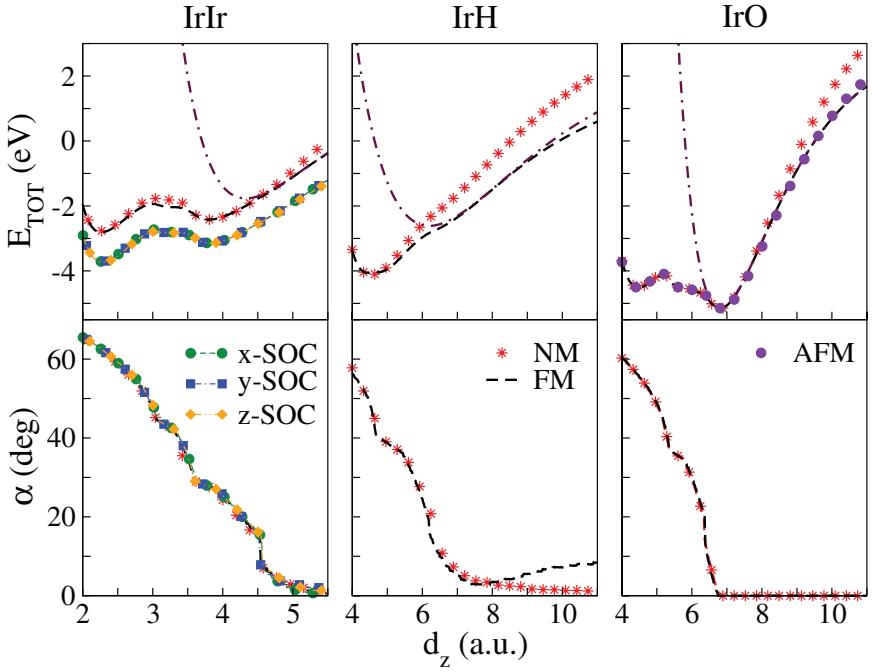

Figure 3. Upper panel: the minimal total energy E_{TOT} (per atom) as a function of the interatomic distance (d_z) for IrIr (left), IrH (middle) and IrO (right). Results of non-magnetic (NM) and ferromagnetic (FM) calculations are presented. For IrIr chains, results when applying spin–orbit coupling are also shown. The dashed–dotted maroon lines correspond to the total energies of the linear infinite FM chains. For IrO, the violet circles stand for the total energy of the antiferromagnetic solution. Lower panel: the evolution of the corresponding zigzag α-angles.

which we extracted the effective minimum energy curves as a function of d_z, $\epsilon(d_z) = \min_{d_x}\epsilon(d_z, d_x)$. Our main results for single-atom Pt and Ir chains are summarized in the left panels of figures 2 and 3, respectively, where the total energies and the zigzag α-angles are plotted as a function of d_z. We obtain the minimum energy curves for different magnetic configurations, namely non-magnetic (NM), ferromagnetic (FM) and including spin–orbit coupling, with the magnetization pointing along three directions of space, namely x-SOC, y-SOC and z-SOC. We present, in figures 2 and 3,

only a selection of the collected data that illustrates the main results, to avoid confusing the reader with too many curves. Total energies of the FM Pt and Ir infinite linear chains are also shown for comparison. We find a characteristic two-well structure in the energy curves for both Pt and Ir, where the first minima are located around 62° for both atomic chains, and the second minima are around 27° in the Pt case and around 28° in the Ir chains, showing that these metals prefer higher coordination and closely packed structures. Our results agree well with those reported by Fernández-Seivane [21, 22] and by Tung [23], except for the location of the second minimum at $\alpha \sim 45°$ in Ir chains found by Fernández-Seivane. It is interesting to note that inclusion of the spin-orbit interaction does not modify the general trends of the energy profiles in any of the studied systems.

To study the effect of the above-mentioned sp-dopants on Pt and Ir chains, we performed non-magnetic and spin-polarized calculations in the scalar relativistic approximation (FM) and included the effect of spin-orbit coupling via Pauli Hamiltonian (SOC). A collection of representative results is presented in the middle and right panels of figures 2 and 3, where we show the total energy curves as well as the evolution of the α-angles as a function of d_z, for Pt-X and Ir-X (X = H,O) chains. We also included the energies of the corresponding infinite linear chains. We find that, when including SOC, the energies are lower than the corresponding FM ones, but the curve's features are similar, giving the same structural properties. The trends observed in the energetics of the NM results are similar to those obtained from the FM calculations. One feature that has to be pointed out is that, in general, we obtain that both Pt and Ir are ferromagnetic, not only in single-atom chains but also with impurities, as can be seen from the upper panels of the figures. This property is enhanced when stretching the atomic chains. Nevertheless, there is a range of d_z values where we obtain that the NM structure is more stable than the FM, when the impurity is s-like. This range is smaller for Pt than for Ir. With respect to the geometric structure, we find that, when including an s-like impurity, the planar zigzag structure is more stable, with $\alpha \sim 40°$ for both Ir and Pt chains. The energy curves in the vicinity of this angle are rather flat. When we introduce a p-like dopant the energy curves are quite different to the ones obtained for the single-atom chains, as the two-well structure is no longer present; instead, a three-minima curve emerges. The global minima are located in d_z, corresponding to linear chains, indicating that the presence of this kind of impurity leads to an effective straightening of the bonds in the chains.

A common feature for all Pt-based chains, which can be seen from comparison between figures 2 and 3, is that their energy curves have smaller slopes than the ones displayed by the Ir-based chains. This softening of the energy profile can be related to the fact that the d_{xy} and $d_{x^2-y^2}$ states of Pt are below the Fermi energy (E_F) whereas in the case of Ir these states are crossing E_F, thus providing an additional channel for hybridization and bonding between the atoms. Similar behavior was also found when comparing Au and Ag chains [15]. This fact has considerable impact on the chain stabilization process, as we will discuss in the next section.

For IrO chains we have also tested the possibility of an antiferromagnetic (AFM) solution (see figure 3). We find that there are two ranges of d_z values where the AFM solution is more stable: namely, for large α values ($4.0\ \text{bohr} < d_z < 4.4\ \text{bohr}$) and when $d_z \in (6.85\ \text{bohr} < d_z < 9.55\ \text{bohr})$. Concerning the geometric structure derived from the features of the energy profiles, there are no substantial differences between the FM and AFM solutions; therefore, we do not consider this magnetic structure when analyzing the chain formation process in the following section. To summarize, we find that structural properties are essentially independent of magnetism or the presence of a spin–orbit interaction.

We turn our attention now to the magnetic properties of the studied chains. In this work, we do not report on magnetic anisotropy energies (MAEs) and orbital moments, as these two quantities, for Pt and Ir chains, have been extensively studied in the past [21–28]. The evolution of the atomic spin moments with d_z is presented in figure 4. In the upper panel we show the spin moments for the Pt–Pt and Pt-X (X = H,O) cases, while in the lower panel the Ir–Ir and Ir-X moments are plotted. In the case of impurities, the metal's magnetic moments are calculated as the unit cell moment minus the local moment of the X atom, as the muffin-tin radii we use are too small to give reasonable values of the magnetic moments of the metal atoms but are big enough to describe the local moment on the X atom. As can be seen in this figure, magnetic moments increase almost monotonically in Pt chains, whereas in the case of Ir chains they show a high-spin to low-spin to high-spin transition in the range of d_z, which corresponds to the formation of the zigzag minimum during stretching. Both cases are magnetic in their ground state zigzag structures, and their magnetic moments at corresponding distances are similar, $\mu_S \sim 0.44\mu_B$. All our calculated magnetic moments agree well with previously reported values [21–24].

Both 5d TMs, when combined with H, show a monotonous increment in their magnetic moments from zero to the saturated value—that which is obtained for the monoatomic wires. Including O in the atomic chains leads to interesting magnetic behavior. In the Pt case, there is a transition between high-spin state and low-spin state, then back to the high-spin state, in contrast to what was observed in the Pt monowire. The same trend is exhibited by the O atoms (not shown). In the Ir case, while the high-spin to low-spin transitions were present in the Ir monowires, they are no longer present when combining Ir with O. In this case, the Ir magnetic moments are negligible until the distance at which a drastic increase in the moment up to very large values starts. The O moments show the same trend, with smaller magnetic moments.

An example of how the ferromagnetic density of states (DOS) evolves, as the parameter d_z increases, is shown in figure 5, in which we refer to some selected cases. In the upper panels the DOS of infinite linear chains, corresponding to small and large Ir–Ir distance, is presented. As can be seen, in the small distance case the exchange splitting is small, giving rise to a magnetic moment of $0.37\mu_B$. When the interatomic distance in the monowires is increased, the tendency to ferromagnetic order and exchange splitting are strongly enhanced,

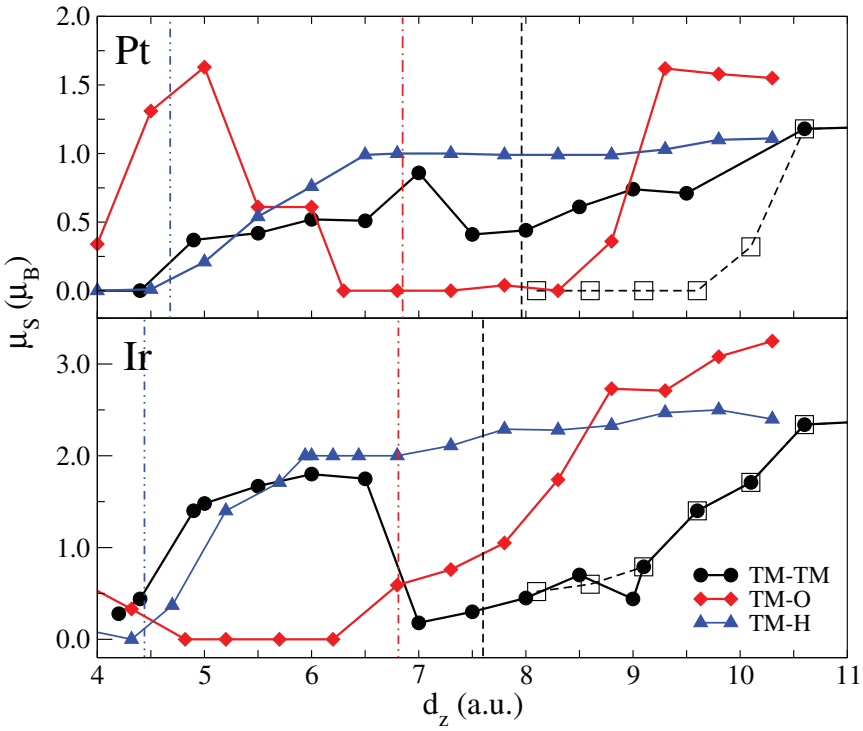

Figure 4. Magnetic moments of the transition-metal atom (in μ_B) as a function of d_z in Pt, Pt-X (upper panel), Ir and Ir-X (lower panel) chains. Open squares correspond to pure 5d-TM linear chains, black circles to pure TM zigzag chains, red diamonds to TM-O chains and blue triangles to TM-H chains. Vertical lines indicate the equilibrium distance of each case (dashed black lines: TM–TM chains, dot–dashed red lines: TM-O chains and dot–dot–dashed blue lines: TM-H chains). For monowires, the double cell is taken into account to enable a comparison at the same distance between all types of chains.

giving rise to huge magnetic moments (see lower panel of figure 4). The cylindrical symmetry present in the linear chains is also verified in the upper panels of figure 5, where the d_{xy} and $d_{x^2-y^2}$ (Δ_4-symmetry) orbitals are degenerate, as well as the d_{zx} and d_{yz} (Δ_3-symmetry) orbitals. These degeneracies are broken when the chain has a zigzag geometry, as can be observed in the DOS of the two different zigzag α-angles presented in the lower panels of figure 5, corresponding to a low-spin ($2d_z$=8 bohr; α=26.6°) and a high-spin ($2d_z$=6 bohr; α=45°). In the high-spin case (lower left) the exchange splitting is large, consistent with high magnetic moments. On the other hand, in the low-spin case (lower right) the exchange splitting is small—but not negligible, giving rise to a small magnetic moment. Note that in all the presented cases, the bigger the Ir–Ir distance d_z, the narrower the bands, due to larger Ir–Ir bonding distances.

4. Producibility and stability of the chains

In this work, we apply the generalization of our model for chain formation in break-junctions [15], based on total energy arguments where zigzag and linear geometries, as well as the presence of impurities, are taken into account.

Before analyzing the results, it is important to discuss the energy scales that determine the elongation process. While the extraction of atoms out of the leads can be modeled in line with previous studies [29, 30], we have also to consider the supplementing of the pure chain with the impurities. Here we assume that the light sp-dopants are present in the atmosphere and are not bound at the surface. This assumption is well-justified, considering that the concentration of such impurities is controlled by the partial pressure in experiments. Here we refer to results by Bahn *et al* [13], who reported a highly preferential binding of impurity atoms to Au chains, allowing an important simplification: impurities have a strong tendency to cover all assisted bonds of the chain atoms. Hence, the resulting structure is well-described as a chain of alternating atoms.

To briefly recall our model, we divide the system into two regions: the leads and the suspended chain. The electronic structure of the two parts is considered separately, thus neglecting their mutual influence. This approximation is good enough to describe the formation of long chains [26, 29], which is the purpose of the current work. Within our model, the whole process of chain formation consists of two consequent processes. First, one atom is extracted out of the lead into the chain, reducing the coordination of this particular atom. This requires additional external energy, which we account for by the difference of the cohesion energy for an atom in the lead, $E_{\rm lead}$, and in the chain, $E_{\rm W}(d_0)$, both at equilibrium distance, thus giving $\Delta E_{\rm lead}=E_{\rm W}(d_0)-E_{\rm lead}$. $E_{\rm lead}$ is calculated as explained in [15] and the values of the energy barriers we use for Pt-based chains are $\Delta E_{\rm lead}$=1.852 eV, 1.791 eV and 1.900 eV for NM, FM and SOC calculations, respectively. The corresponding ones for Ir-based chains are $\Delta E_{\rm lead}$=2.809 eV, 2.684 eV and 2.693 eV.

The second process is related to the relaxation of all the chain bonds to a smaller interatomic distance after the

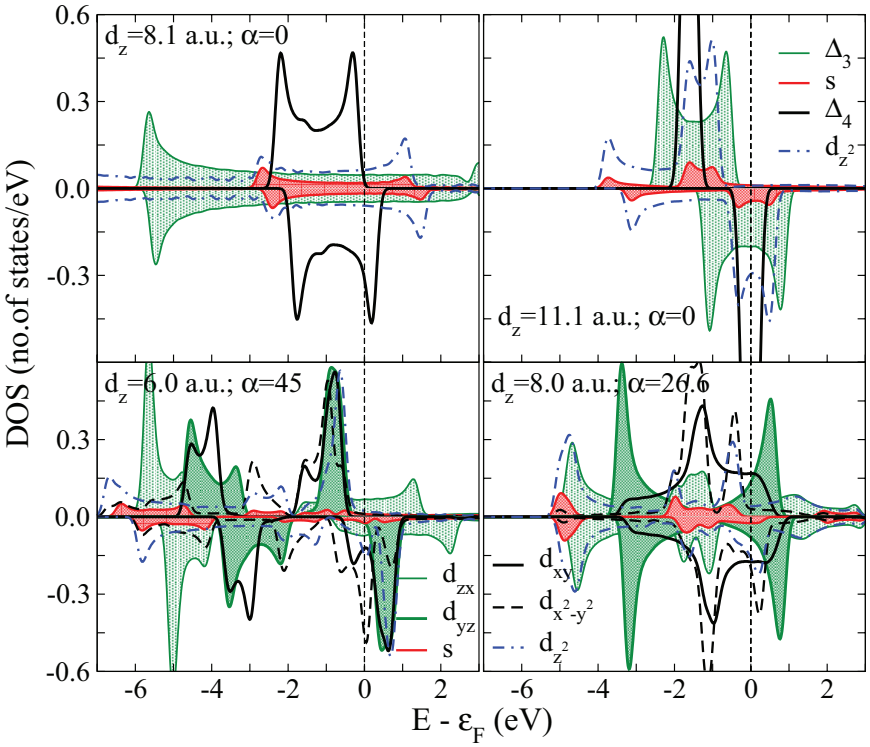

Figure 5. Orbital decomposition of the density of states of pure Ir chains in selected geometries. Upper panel: linear chains with two different Ir–Ir distances. Low-spin (left) and high-spin (right) examples are shown. Lower panel: two different Ir zigzag chains. High-spin (left) and low-spin (right) examples are plotted. The Ir monowire double cell is taken into account to facilitate the comparison with figure 4. The vertical black line represents the Fermi energy (ϵ_F). For linear chains the d_{xy} with $d_{x^2-y^2}$, and d_{zx} with d_{yz} can be grouped into Δ_4 and Δ_3 states, respectively.

additional atom has entered the chain. In this way, the chain formation process can be translated into the following equation (P-criterion):

$$E^*(d, N) = (N+1)\,\epsilon(d) - [\Delta E_{\text{lead}} + (N+2)\,\epsilon(\tilde{d})] \quad (1)$$

where $d = L/(N+1)$ and $\tilde{d} = L/(N+2)$ are the chain interatomic distances before and after the elongation, respectively: $N+1$ is the number of bonds in a chain of N atoms and L is the distance between the leads. The binding energy of the suspended chain, $\epsilon(d)$, is defined from the binding energy of the infinite wire, with interatomic distance d, $E_W(d) = E_W(d_0) + \epsilon(d)$, relative to the wire's cohesive energy at equilibrium interatomic distance d_0, $E_W(d_0)$, which implies $\epsilon(d) > 0$.

If $E^*(d, N) > 0$ the P-criterion is satisfied and the chain can increase by one atom for that particular pair of parameters (d, N). To apply the P criterion to suspended chains, we fit the wire-binding energy $\epsilon(d)$ by interpolating the minimum energy curve from the binding energy of several d_x and d_z distances [15]. Thus, the binding energies participating in equation (1) are the ones depicted in figures 2 and 3. To analyze the criterion, we plot the energy $E^*(d, N)$ surface (P-area, in what follows) for several selected cases, as shown in figure 6, where we also included the energy landscape of single-atom Pt linear chains for better comparison. We do not show the P-areas for all considered magnetic configurations, to avoid confusing the reader with too many plots. The area of the phase space where $E^* > 0$ provides the parameters for which the elongation by one atom (or one pair of atoms when the impurities are considered) is probable. This probability is greater for higher values of E^*, given by the color-coding in the figure.

One of the most distinct differences visible, when comparing linear and zigzag single-atom chains, is that two different areas of positive E^* appear when considering zigzag geometry. This suggests that, in an experiment, the coexistence of these phases can enhance the elongation properties of the chains by switching from the linear region of producibility into the zigzag one. This could be achieved by pushing the tips towards each other, therefore reducing the interatomic distance in the chain that allows the zigzag geometry to be stabilized. This interesting and useful property is one of the most important outcomes of our extended model, as we are taking into account the relaxation at short interatomic distances into zigzag geometries which are energetically favorable. It is important to mention that, when analyzing the incidence of magnetism and spin orbit interaction (not shown) in the P-area, we do not find any substantial changes in the shape and position of the P-regions, compared to the non-magnetic situations without spin–orbit. This can be seen from the second and third panels of figure 6. Noticeably, it is only the value of E^* which is affected by magnetism, being 1–2 eV smaller for magnetic chains than for the non-magnetic ones. This reduction is a direct consequence of the change in the energy profile and corresponding breaking force (see e.g. figure 3 and table 1) upon taking spin-polarization into account. Generally, the effect of the reduced probability for

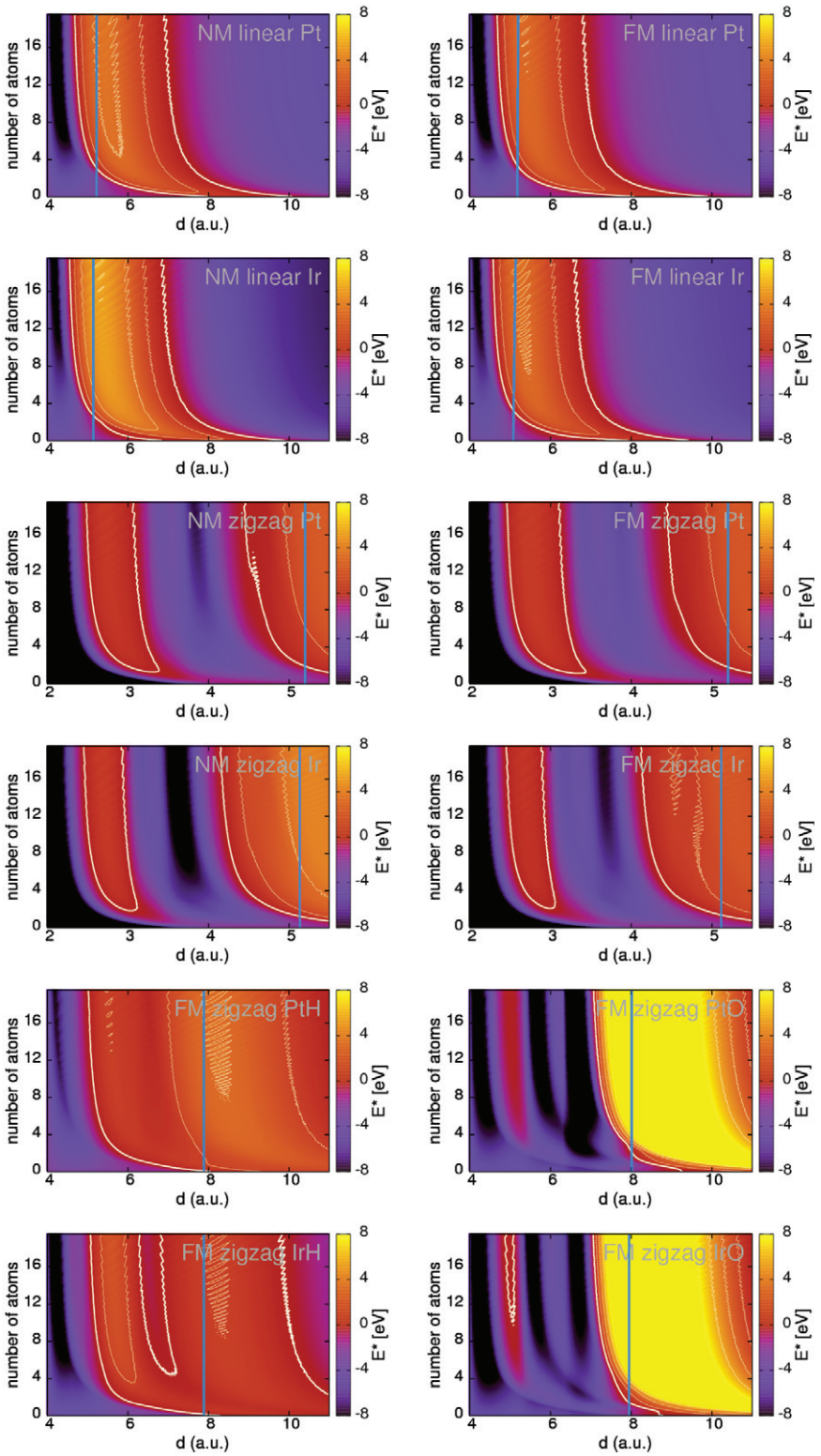

Figure 6. Selected energy landscapes $E^*(d, N)$ as a function of interatomic distance (d) and number of atoms in the chain (N) describing the chain producibility for pure and impurity-assisted Pt and Ir chains, where E^* is defined by the criterion for producibility, (equation (1)). Thick white lines mark the $E^* = 0$ isolines indicating regions of producibility ($E^*(d, N) > 0$). Additional thin isolines are drawn at $E^*(d, N) = 2$ eV, 4 eV, 6 eV, and 8 eV in each panel. Note that regions which are outside of the interval [−8 eV, 8 eV] are shown in the same color-coding as the minimal and maximal value of this interval. To rate the stability of chains, for each panel the inflection point $\hat{d}$ in the linear regime of the binding energy potential is depicted by thick blue vertical lines.

Table 1. Calculated break forces, F_0 (eV/a.u.). The F_0 value that corresponds to the easy-axis at the breaking point when including SOC is shown in bold.

Case	NM	FM	x, y-SOC	z-SOC
PtPt	1.33	1.24	1.16	**1.14**
PtH	1.05	1.03	1.04	**1.03**
PtO	2.35	2.22	**2.16**	2.18
IrIr	1.91	1.51	1.43	**1.37**
IrH	1.12	0.91	1.02	**1.02**
IrO	2.69	2.38	2.38	**2.30**

producibility in magnetic systems is in accord to [30]. On the other hand, the effect of the spin–orbit interaction on the producibility of the chains is even less pronounced.

The main differences in the P-areas are obtained when introducing environmental impurities into the chain formation process (see the last two panels of figure 6). For both 5d TMs chains, we can see that, when including H in the chains the P-area becomes significantly wider, as compared to the pure linear and zigzag chains. This can be attributed to the fact that, in TM-H chains, there is only one stable zigzag phase with a rather flat minimum: the chains are stable for a rather broad range of α angles. Nevertheless, even if with H impurities the chains are producible in a wider range of d_z distances, they are more likely to grow if O is the impurity which assists the chain growth—as follows from the larger values of E^* (see color coding of figure 6).

To test the stability of the chains, we turn to the string tension, $F(d)$, which is defined as the slope of the binding energy with respect to the distance between the atoms along the z-axis, i.e. $F(d)=F(d_z)=\delta\,\epsilon(d_z)/\delta d_z$. The maximum of this quantity, the so-called 'break force' $F_0=F(\widehat{d})$ can give us a very rough estimate of how far an ideal infinite chain can be stretched until it breaks at a distance $\widehat{d}$, indicated with thick blue vertical lines in figure 6. As we are dealing not only with linear monowires but also with planar zigzag wires, in the energy binding curve we find more than one minimum. In general, the minima located at lower distances d_z are the ones corresponding to zigzag geometries and, therefore, the chains are not under high tension in this region. The minima that are located at higher distances correspond to the elongation situation, and so it is in this region where the chain can be broken if the break force is applied. Physically, a successful chain elongation event will occur when the following happens: as the chain is stretched, the energy of the system increases up to the point where a lead atom overcomes the chain formation barrier, ΔE_{lead}, and enters the chain. This reduces the distance in the chain from d to $\widetilde{d}$ and lowers the total energy of an atom in the wire, $E_{\mathrm{W}}(\widetilde{d})<E_{\mathrm{W}}(d)$. The larger the slope of the total energy $E_{\mathrm{W}}(d)$, the more energy can be gained by relaxing the chain from a distance d to $\widetilde{d}$. Therefore, large values of F_0 and small energy barriers ΔE_{lead} will favor chain elongation.

In table 1 we show calculated break forces, F_0, for the systems we studied. As a general rule, we observe that non-magnetic calculations lead to enhanced stability of the chains, in agreement with previous results [21, 22, 30]. When comparing the break forces for all the studied cases we first note that in pure chains a stronger binding, and correspondingly larger values of F_0, occur for Ir: a direct consequence of the smoother energy profile of Pt chains, discussed in section 3. Introducing s-like impurities leads to lower F_0 values, contrary to what is obtained for Cu, Ag and Au chains (see [15]), where s-like impurities help to strengthen the bonds. This can be attributed to the fact that the presence of H in the chains, on the one hand, causes the smallest strengthening of the bonds due to the absence of directionality of the s-orbitals but, on the other hand, increases the magnetic moments of the metal atoms, thus impeding the formation of long chains in break junctions, according to the mechanism discussed in [30]. Furthermore, when the chains are assisted by p-like impurities, more pronounced directionality of the covalent bonds leads to considerably bigger values of the corresponding break forces.

5. Conclusions

In this work we have applied the generalization of the chain formation model presented in [15] to two late 5d-TMs chains, Pt and Ir, with two prototype impurities: the s-like and p-like impurities (H and O, respectively). The geometrical extension of the model is essential to describe assisted-chain creation, but also leads to a quantitative refinement of the predicted interchain distances during the chain creation process of the pure chain. We have investigated the growth probability and stability of the wires, taking the input from first-principles calculations. We find that neither magnetism nor spin–orbit interaction play a crucial role in the structural properties of the atomic chains, but they do play a role in their producibility and stability in break junction experiments as the absence of magnetism leads to an enhanced stability. We also find that Ir chains are more likely to form than Pt chains, and that O-assisted chain growth leads to a strongly enhanced tendency towards chain elongation, when compared to pure chains. On the other hand, the presence of H-impurities increases the spin magnetic moments of the metal atoms, resulting in a smaller break force and reduced structural stability.

Acknowledgments

YM gratefully acknowledges funding under the HGF-YIG Programme VH-NG-513 and SDN acknowledges funding from Conicet, PIP00258. SDN acknowledges funding from Conicet, PIP00258, PIP11220120100069CO, and from MINCyT, PICT 2011–1187.

References

[1] Smit M R H, Untiedt C, Yanson A I and van Ruitenbeek J M 2001 *Phys. Rev. Lett.* **87** 266102
[2] Ryu M and Kizuka T 2006 *Japan. J. Appl. Phys.* **45** 8952
[3] Ohnishi H, Kondo Y and Takayanagi K 1998 *Nature* **395** 780
[4] Yanson A I, Rubio G, van Brom H E, Agraït N and van Ruitenbeek J M 1998 *Nature* **395** 783
[5] Rubio-Bollinger G, Bahn S R, Agraït N, Jacobsen K W and Vieira S 2001 *Phys. Rev. Lett.* **87** 026101

[6] Hirjibehedin C F, Lutz C P and Heinrich A J 2006 *Science* **312** 1021
[7] Lucignano P, Mazzarello R, Smogunov A, Fabrizio M and Tosatti E 2009 *Nature Mater.* **8** 563
[8] Calvo M R, Fernández-Rossier J, Palacios J J, Jacob D, Natelson D and Untied C 2009 *Nature* **458** 1150
[9] Khajetoorians A A *et al* 2013 *Science* **339** 55
[10] Dasa T R, Ignatiev P A and Stepanyuk V S 2012 *Phys. Rev.* B **85** 205447
[11] Barnett F D, Haekkinen H, Scherbakov A G and Landman U 2004 *Nano Lett.* **4** 1845
[12] Novaes F D, da Silva A J R, da Silva E Z and Fazzio A 2006 *Phys. Rev. Lett.* **96** 016104
[13] Bahn S R, Lopez N, Norskov J K and Jacobsen K W 2002 *Phys. Rev.* B **66** 081405
[14] Thijssen W H A, Marjenburgh D, Bremmer R H and van Ruitenbeek J M 2006 *Phys. Rev. Lett.* **96** 026806
[15] Di Napoli S, Thiess A, Blügel S and Mokrousov Y 2012 *J. Phys.: Condens. Matter* **24** 135501
[16] Aradhya S V, Frei M, Halbritter A and Venkataraman L 2013 *ACS Nano* **7** 3706
[17] Novaes F D, da Silva A J R, da Silva E Z and Fazzio A 2003 *Phys. Rev. Lett.* **90** 036101
[18] Rodrigues V, Bettini J, Rocha A R, Rego L G C and Ugarte D 2002 *Phys. Rev.* B **65** 153402
[19] Mokrousov Y, Bihlmayer G and Blügel S 2005 *Phys. Rev.* B **72** 045402
[20] FLEUR: The Julich FLAPW code family 2014 www.flapw.de
[21] Fernández-Seivane L, García-Suárez V M and Ferrer J 2007 *Phys. Rev.* B **75** 075415
[22] García-Suárez V M, Manrique D Z, Lambert C J and Ferrer J 2009 *Phys. Rev.* B **79** 060408
[23] Tung J C and Guo G Y 2010 *Phys. Rev.* B **81** 094422
[24] Delin A and Tosatti E 2003 *Phys. Rev.* B **68** 144434
[25] Smogunov A, Dal Corso A, Delin A, Weht R and Tosatti E 2008 *Nature Nanotechnol.* **3** 22
[26] Thiess A, Mokrousov Y and Heinze S 2010 *Phys. Rev.* B **81** 054433
[27] Negulyaev N N, Dorantes-Dávila J, Niebergall L, Juárez-Reyes L, Pastor G M and Stepanyuk V S 2013 *Phys. Rev.* B **87** 054425
[28] Di Napoli S, Thiess A, Blügel S and Mokrousov Y 2014 to be submitted
[29] Thiess A, Mokrousov Y, Blügel S and Heinze S 2008 *Nano Lett.* **8** 2144
[30] Thiess A, Mokrousov Y, Heinze S and Blügel S 2009 *Phys. Rev. Lett.* **103** 217201